ASSOCIAZIONE NAZIONALE ITALIANA DI INGEGNERIA SISMICA
ANIDIS
Italian National Association of Earthquake Engineering

XVIII CONVEGNO ANIDIS
L'ingegneria sismica in Italia
ASCOLI PICENO 2019
15-19 Settembre

Field tests on a soil-foundation-structure system subjected to scour

Enrico Tubaldi[1], Rosa Lupo[1], Stergios Mitoulis[2], Sotiris Argyroudis[2], Fabrizio Gara[3], Laura Ragni[3], Sandro Carbonari[3], Francesca Dezi[4]

[1] *Department of Civil and Environmental Engineering, University of Strathclyde, 75 Montrose Street, Glasgow G1 1XJ, Scotland, United Kingdom*

[2] *Department of Civil and Environmental Engineering, University of Surrey Stag Hill, Guildford GU2 7XH, United Kingdom*

[3] *Department of Construction, Civil Engineering and Architecture, Polytechnic University of Marche, Via Brecce Bianche, 60131, Ancona, Italy*

[4] *Department of Economics, Science and law, University of San Marino, Via Consiglio dei Sessanta, 99, 47891 Republic of San Marino*

Keywords:Bridge scour; Soil-structure Interaction; Impedances; forced-vibrations

ABSTRACT

Earthquakes and foundation scour are the major causes of bridge failure worldwide. Many bridges in earthquake-prone countries have shallow foundations, whose stability and seismic vulnerability can be significantly undermined by flood-induced scour.

This article provides the first results of the "DYMOBRIS" project (DYnamic identification and MOnitoring of scoured BRIdgeS under earthquake hazard), a H2020-SERA EU-funded project aiming at i) developing a methodology for non-invasive detection of scour in bridges with shallow foundations based on vibration monitoring, and ii) quantifying the effects of scour on the seismic vulnerability of these Soil-Foundation-Structure (SFS) systems. The experimental campaign involves various tests, from ambient vibration to force vibration, on the EuroProteas prototype under different scour conditions.

The preliminary finite element models developed for defining the scour profile to be imposed in the in-field tests are presented here, together with some results concerning the effects of scour on the SFS dynamic properties.

1 INTRODUCTION

Earthquakes and foundation scour are the major causes of bridge failure worldwide. Many bridges in earthquake-prone countries have foundations in water, whose stability can be significantly undermined by flood-induced scour (Guo 2014, Yilmaz et al. 2016, Argyroudis et al. 2019) leading to increased seismic vulnerability.

Foundation scour can be defined as the removal of sediments surrounding underwater foundations due to water flow and turbulence (Melville 2000, Tubaldi et al. 2017). This phenomenon has two main effects on bridges: loss of foundation carrying capacity, and increased flexibility of the Soil-Foundation-Structure (SFS) system. The effects of scour can be particularly significant for bridges with shallow foundations, which are very sensitive to the modification of support conditions and bearing capacity reduction induced by scour (see e.g. Zampieri et al. 2017, Tubaldi et al. 2018). Moreover, many bridges exposed to the scour hazard are also located in earthquake-prone countries. It is well known that the overall response of bridges to dynamic loads such as those induced by earthquakes is influenced by Soil-Structure Interaction (SSI) effects (Mylonakis et al. 2006, Carbonari et al. 2017, Carbonari et al. 2011, Dezi et al. 2012). Thus, scour can alter this response, by affecting both the kinematic and inertial soil-structure interaction (Guo 2014) and also by increasing modal periods.

Although many bridges and other critical infrastructure assets exposed to scour (e.g. offshore wind turbines) have superficial foundations, there are no experimental studies in this regard, while most of the research has focused on bridges with deep foundations (Zhang et al. 2017, Liang et al. 2017). Recently, the authors of this paper were awarded a SERA project entitled "DYMOBRIS- Dynamic identification and Monitoring of scoured BRIdgeS under earthquake hazard" (2019). The aim of the project is to fill the gap of knowledge on the dynamic behaviour and seismic performance of bridges with shallow foundations subjected to scour. For this purpose, full-scale tests, from ambient vibrations to force-

vibrations, will be carried out on the EuroProteas SFS system at Euroseistest (Figure 1) to evaluate the effects of foundation scour on the dynamic properties, i.e. frequency and damping, of a Soil-Foundation-Structure (SFS) system.

Figure 1. A photograph of EuroProteas.

This paper illustrates the preliminary numerical analyses carried out to design the experimental full-scale tests in order to predict effects of scour on the foundation stability and the variations of the SFS dynamic properties. For this purpose, a three-dimensional finite element model of the EuroProteas SFS system (Manakou et al. 2010, Pitilakis et al. 2018) has been developed in the Finite Element code Abaqus (2014). In particular, various models are built, namely the Fixed Base (FB) structure, the structure with the soil-foundation system modelled using linear springs and dashpots which simulate impedance functions, and the structure with a continuous soil domain.

2 TESTING FACILITY DESCRIPTION

This section describes the geometrical and mechanical properties of the EuroProteas SFS system. This system consists of four steel column, eight steel X-braces, and three reinforced concrete slabs. The two slabs placed at the top of the columns represent the superstructure mass, whereas the one at the bottom represents the shallow foundation, resting on the soil. The total height of the system is 5.0 m from the bottom of the foundation slab to the top of second roof slab, whereas its total mass is approximately 28.2 ton. The columns have QHS sections with dimensions of $150x150x10$ mm and length 3.80 m. The steel X-braced are L-shaped with section $100x100x10$mm. Each slab is $3.0x3.0x0.40$ m, and was cast with concrete, using steel reinforcement of 14 mm in diameter.

The stratigraphy and dynamic properties of the soil are well-documented from extended geotechnical and geophysical surveys reported in earlier studies (Manakou et al. 2010, Pitilakis et al. 2018). The upper 5m layers consist of silty sands, with an average shear wave velocity V_s = 130 m/s and a density ρ = 1.87 ton/m^3. Based on standard penetration tests, the friction angle of the upper layer was found equal to $\phi' = 32.6°$ and the cohesion $c' = 3\ kPa$. For further details about the structure, the stratigraphy and the dynamic properties of the soil see Pitilakis et al. (2018).

3 NUMERICAL MODELS

This section describes the preliminary numerical models of the EuroProteas SFS system employed for estimating the effects SSI after scour. The three models discussed in the introduction share the same description of the superstructure (Figure 2), with two-nodes linear beam elements used to model the columns and the braces, and 20-node quadratic brick elements used to model the slabs. The columns are connected to the slabs using multi-point tie constraints, whereas the X-braces are connected to the column ends via a hinge connector. Finally, the connections between the two X-braces are based on joint connectors.

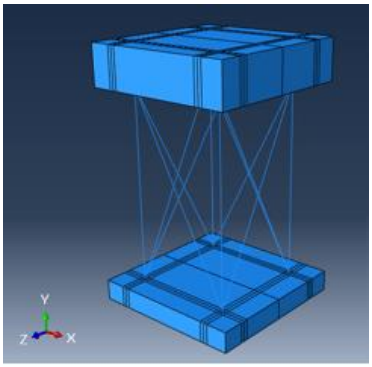

Figure 2 Superstructure used in fixed-base model.

The steel Young's modulus and Poisson's ratio are $E_s = 210000\ MPa$ and $v_s = 0.3$, respectively, whereas the concrete mechanical properties are $E_c = 29962\ MPa$ and $v_c = 0.2$. In addition, a 1% damping factor is assigned to both materials by using the following Rayleigh model. The Rayleigh damping coefficient are calibrated to achieve the target damping factor in correspondence of the first and the third modes of vibration of the system, characterized by the highest participation of the superstructure masses along the *x* direction.

The FB model is obtained by restraining the displacements at the base of the foundation slab. This model, characterized by a fundamental vibration frequency of 9.26 Hz (Table 1), is used to estimate the effects of SSI on the vibration properties by comparison with the other two models, namely the one with linear springs and dashpots and the one with the soil considered as a continuum. In the next subsection, these two SFS models are described more in detail and denoted as SFS_1 and SFS_2, respectively.

Table 1. Resonant frequencies for different structural configuration (case with no scour).

Structural configuration	Resonant frequency [Hz]	
	Abaqus	Experimental
FB model	9.26	-
SFS_1 model	4.48	4.1
SFS_2 model	4.22	4.1

3.1 Structure with soil modelled using a simplified impedance function model

In this model, the semi-infinite soil-domain is replaced by a set of distributed springs and dampers with the aim of obtaining a simplified description of the SSI problem. This approach is similar to the one followed in Tubaldi et al. (2018) and Ragni et al. (2019), with zero-thickness cohesive interface elements resisting only compression stresses at the bottom of the foundation describing the soil reaction. The cohesive interface elements have a visco-elastic behaviour, with properties based on the work of Gazetas (1991).

The springs constants (stresses per unit displacements) have been evaluated as follows:

$$k'_{s,x} = \frac{k_{s,x}}{A_x},\ k'_{s,y} = \frac{k_{s,y}}{A_y},\ k'_{s,z} = \frac{k_{s,z}}{A_z} \tag{1}$$

where $k_{s,x}$, $k_{sh,y}$ and $k_{sh,z}$ are given by Gazetas (1991) as a function of the shear module, $G=V_s \cdot \rho^2 = 31.47\, N/mm^2$, the Poisson's ratio, ν=0.4, and of the foundation geometry, whereas A is the foundation area in contact with the soil.

The dashpots are in parallel with the springs and represent the soil radiation damping according to the following expression (Gazetas 1991):

$$c'_x \simeq (\rho V_s) \cdot \tilde{c}_x\ ,\ c'_z = (\rho V_s) \cdot \tilde{c}_z\ ,$$
$$c'_y = (\rho V_{La}) \cdot \tilde{c}_y \tag{2}$$

where ρ is material's density, V_{La} is Lysmer's shear wave velocity, related to V_s, and $\tilde{c}_x$, $\tilde{c}_y$ and $\tilde{c}_z$ are function of the foundation's geometry and mechanical soil properties. A 5% damping factor is added to reflect the soil hysteretic damping. In this work, it is assumed that the damping does not change with frequency, and the values of , $\tilde{c}_x$, $\tilde{c}_y$ and $\tilde{c}_z$ are those corresponding to the system natural frequency. The values of the subgrade reactions are $k'_{s,x} = 0.0295\ N/mm^3$, $k'_{s,z} = 0.0295\ N/mm^3$, and $k'_{s,y} = 0.0397\ N/mm^3$. The values of the damping coefficients (including the hysteretic component) are $c'_x = 3062.4\ N \cdot s/mm$, $c'_z = 3062.4\ N \cdot s/mm$, and $c'_y = 4932.2\ N \cdot s/mm$.

To simulate scour in Abaqus, the "model change" capability is employed, allowing to progressively eliminate the cohesive interface elements at the foundation-soil interface that represent the portion of eroded soil.

3.2 Soil model with absorbing boundaries

This sub-section describes the three-dimensional model including the semi-infinite soil-domain. This domain is modelled with solid elements with elasto-plastic behaviour. The elastic soil behaviour is described by assigning $G = 31.47\ N/mm^2$ and $\nu = 0.4$. The plastic behaviour is defined by the Mohr-Coulomb model, with a friction angle $\Phi' = 32.6°$, dilatation angle $\varphi = 2.6°$, and cohesion $c' = 0.003\ MPa$. The soil material damping is described trough the Rayleigh formula, with a damping ratio of 5%.

The interaction between the foundation and the soil is modelled using the "surface to surface" contact approach. The interface has a very high stiffness in compression to avoid penetration, can resist only compressive forces, and has a friction coefficient $\mu = 0.6$ along the tangential direction.

The soil is represented by a finite domain with local Absorbing Boundary Conditions (ABCs) to avoid reflection of outgoing waves (Figure 3). The length of the solid domain from the foundation slab outwards is 18m; the absorbing elements are infinite brick elements, and their length is equal to that of the soil domain.

In order to accurately model wave propagation, the mesh size satisfies the following relation (Kuhlemeyer and Lysmeret 1973):

$$l_{max} \leq \left(\frac{1}{8} \sim \frac{1}{5}\right) \lambda_{min} \leq \frac{V_{s,min}}{8 f_{max}} \tag{3}$$

where l_{max} is the maximum element size, λ is shear wavelength, equal to 13 m, $V_{s,min}$ is the shear-wave velocity, equal to $130\ m/s$, and f_{max} = 10 Hz is the maximum frequency of interest.

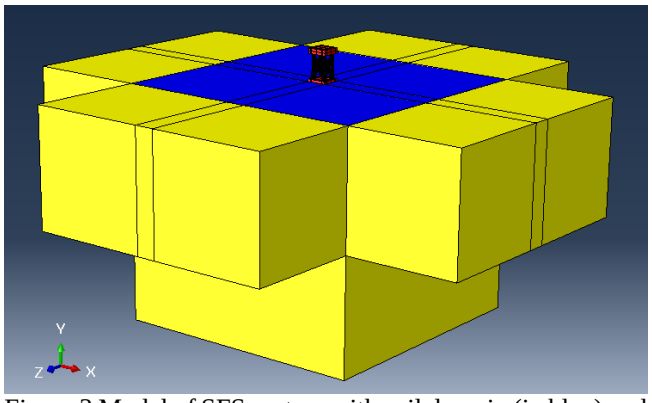

Figure 3 Model of SFS system with soil domain (in blue) and ABCs (in yellow).

4 NUMERICAL RESULTS

This section illustrates the results of the simulation of the response of the structure under several load and scour conditions. For each model and scour condition considered, a static analysis is firstly carried out under the dead loads of the system. Then, a steady-state analysis is performed to simulate the effects of forced-vibrations imposed by the forces applied through a shaker placed on the roof slab. Finally, the Frequency Response Function (FRF), expressing the relationship between the input force and the output displacement at the top slab, is evaluated. This is used to estimate the resonant frequency of the system, f_R, corresponding to the peak of the FRF, and the damping ratio, which is obtained through the half-power bandwidth method.

The amplitude F of the harmonic force applied through the shaker for each excitation frequency is governed by the following equation:

$$F = E(2\pi f)^2 \quad (4)$$

where F is in N, E is the total eccentricity of the shaker (in $kg \cdot m$) and f is the rotational speed of the shaker (in Hz) (Pitilakis et al. 2018).
It is noteworthy that some experiments were already carried out on the EuroProteas system considering an intact foundation (no scour) (Pitilakis et al. 2018). The results of these tests, carried out for a shaker eccentricity E = 1.85 kg-m, are used in this study to validate the proposed numerical models, by comparing the estimates of the resonant frequency with the experimental ones.

4.1 Model with impedance functions

Figure 4 plots the variation with the excitation frequency of the steady state response (output only) obtained by simulating the forced-vibration test (see Table 2) on the model implementing the impedance functions to describe the SSI. The frequency value corresponding to the peak of the corresponding FRF, reported in Table 1, is equal to 4.48 Hz. This value is significantly lower than the one of the fixed base structure (9.26 Hz), demonstrating the high influence of SSI effects on the system response. Moreover, it is slightly higher than the one evaluated experimentally (4.1Hz). The difference between the experimental and numerical estimates may be due to the simplifications inherent to the impedance model, and the fact that the impedance function have been spreaded uniformly along the foundation base. The numerical estimate of the peak displacement is equal to x_{max}= 1.13 mm and the estimated damping ratio is equal to ξ= 4.55%.

In order to evaluate the influence of scour on the SFS dynamic properties, the cohesive interface elements located below a portion of the foundation of width 575 mm along the x direction, from the right extreme of the slab towards the center, are progressively removed in a time history analysis, before performing the steady-state forced-vibration analysis. It can be observed in Figure 4 that scour results in a shift of the FRF peak towards lower frequencies, and an increase of the peak value, due to the reduced stiffness and damping of the system. In particular, in presence of scour the resonant frequency is equal to 3.67 Hz, the peak displacement is equal to 1.30 mm and the the damping ratio increases from the value of 4.55% in the case of no scour to 7.50%.

4.2 Model with continuous soil domain

Figure 4 shows the variation with the frequency of the input of the steady state displacement response obtained for the model including the soil domain. The steady-state response is very close to the one evaluated experimentally, with a similar value of the resonant frequency (4.22 Hz instead of 4.1 Hz). The peak displacement is equal to 1.26 mm, and the damping ratio is equal to 4.76%.

When scour was present, the resonant frequency is equal to 3.27 Hz, the peak displacement is equal to 2.75 mm, and the damping ratio is equal to 6.25%. Thus, the trend of variation of these parameters due to scour is similar to then one observed for the previous simplified model with impedance functions. However, the frequency shift and amplitude increase is much higher in the case of the model with continuous soil domain.

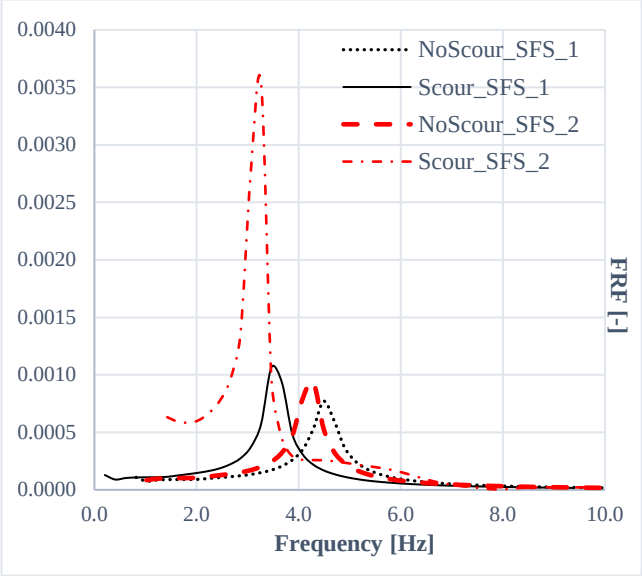

Figure 4. FRF for model with impedance function (SFS_1) and with continuous soil domain (SFS_2).

5 CONCLUSIONS

This paper presented some preliminary results of an experimental and numerical study aimed at evaluating the influence of scour on the dynamic behaviour of a system with shallow foundation.
Three different models of the EuroProteas system have been developed in Abaqus. The first one is the fixed-based frame, whereas the other two simulate the interaction with the soil by means of impedance functions or by including the soil domain in the FE model and using absorbing elements at the boundaries. These models allowed to investigate the effect of soil-structure interaction and of scour. In particular, it is observed that scour results in a decrease of the frequency of vibration of the system, an increase of the peak response, and a reduction of the damping ratio of the system. These effects are the result of the increased flexibility of the system and the reduced capabilities of the system to dissipate energy through radiation in the soil.

The proposed modelling strategy will be a-posteriori validated by comparing results with experimental data obtained from tests carried out on the EuroProteas, and will be used to quantify the influence of scour on the kinematic and inertial interaction of bridges with scoured foundations.

REFERENCES

Argyroudis S., Mitoulis S.A., Winter M., Kaynia A.M., 2019. Fragility of transport assets exposed to multiple hazards: State-of-the-art review toward infrastructural resilience. *Reliability Engineering and System Safety* (*in press*), https://doi.org/10.1016/j.ress.2019.106567.

Carbonari S., Dezi F., Leoni G., 2011. Seismic soil-structure interaction in multi-span bridges: Application to a railway bridge. *Earthquake Engineering and Structural Dynamics*, **40**(11), 1219-1239.

Carbonari S., Morici M., Dezi F., Gara F., Leoni G., 2017. Soil-structure interaction effects in single bridge piers founded on inclined pile groups. *Soil Dynamics and Earthquake Engineering*, **92**, 52-67.

Dezi F., Carbonari S., Tombari A., Leoni G. 2012. Soil-structure interaction in the seismic response of an isolated three span motorway overcrossing founded on piles. *Soil Dynamics and Earthquake Engineering*, **41**, 151-163.

DYMOBRIS - Dynamic identification and Monitoring of scoured BRIdgeS under earthquake hazard. Reference: 730900. SERA, Call: H2020-INFRAIA-2016-1.

Gazetas, G., 1991. Formulas and charts for impedance of surface and embedded foundations. *Journal of geotechnical engineering*, **117**(9), 1363-1381.

Guo, X., 2014. *Seismic vulnerability analysis of scoured bridge systems.* PhD Thesis, University of Missouri-Kansas City.

Hoffmans, G. J. C. M., Verheij, H. J., 1997. Scour manual. Balkema, Rotterdam, Netherlands.

Kuhlemeyer, R. L., Lysmer, J., 1973. Finite element method accuracy for wave propagation problems. *Journal of the Soil Dynamics Division*, **99**, 421-427.

Manakou, M., Raptakis, D., Chávez-García, F. J., Apostolidis, P., Pitilakis, K., 2010. 3D soil structure of the Mygdonian basin for site response analysis. *Soil Dynamics and Earthquake Engineering*, **30**(11),1198–211.

Melville, B. W., Coleman, S. E., 2000. Bridge scour. Highlands Ranch, Colorado, USA: *Water Resources Publications*.

Mylonakis, G., Nikolaou, S., Gazetas, G., 2006. Footing under seismic loading: Analysis and design issuses with emphasis on bridge foundations. *Soil Dynamics and Earthquake Engineering*,**26**(9), 824-853.

Nielsen, A. H., 2006. Absorbing Boundary Conditions for Seismic Analysis in ABAQUS. *ABAQUS Users'Conference.*

Pitilakis, D., Rovithis, E., Anastasiadis, A., Vratsikidis, A., Manakou, M., 2018. Field evidence of SSI from full-scale structure testing. *Soil Dynamics and Earthquake Engineering*, **112**, 89-106.

Ragni, L., Scozzese, F., Tubaldi, E, Gara, F. Dynamic properties of a masonry arch bridge subjected to local scour. *2nd International Conference on Natural Hazards & Infrastructure ICONHIC 2019*, June 23 – 26 2019, Chania, Greece.

Tubaldi, E., Macorini, L., Izzuddin, B. A., 2018. Three-dimensional mesoscale modelling of multi-span masonry arch bridges subjected to scour. *Engineering Structures*, **165**, 486-500.

Tubaldi E., Macorini L., Izzuddin B.A., Manes C., Laio F, 2017. A framework for probabilistic assessment of clear-water scour around bridge piers. *Structural safety*, **69**, 11-22.

Yilmaz, T., Banerjee, S., & Johnson, P. A, 2016. Performance of two real-life California bridges under regional natural hazards. *Journal of Bridge Engineering*, **21**(3), 04015063.

Zampieri, P., Zanini, M.A., Faleschini, F., Hofer, L., Pellegrino, C., 2017. Failure analysis of masonry arch bridges subject to local pier scour. *Engineering Failure Analysis*, **79**, 371–84.